Journal of Alloys and Compounds 800 (2019) 191–197

Contents lists available at ScienceDirect

Journal of Alloys and Compounds

journal homepage: http://www.elsevier.com/locate/jalcom

The role of samarium incorporated structural defects in ZnO thin films prepared by femtosecond pulsed laser deposition

Jaweria Zartaj Hashmi [a, b, *], Khurram Siraj [a], Anwar Latif [a], Shahzad Naseem [c], Mathew Murray [b], Gin Jose [b]

[a] Laser and Optronics Centre, Department of Physics, University of Engineering and Technology, Lahore 54890, Pakistan
[b] Applied Photon Science, School of Chemical and Process Engineering, University of Leeds, Leeds LS2 9JT, UK
[c] Centre of Excellence in Solid State Physics, University of the Punjab, Lahore 54590, Pakistan

ARTICLE INFO

Article history:
Received 16 March 2018
Received in revised form
21 May 2019
Accepted 29 May 2019
Available online 30 May 2019

Keywords:
PLD
ZnO
Microstructure
AFM
Optical band gap
Luminescence
Electrical resistivity

ABSTRACT

Samarium, a rare-earth element is used as an impurity in ZnO to study the effects it causes in structure thereby changing the optical and electrical characteristics of ZnO thin films. Samarium zinc oxide ($Sm_xZn_{1-x}O$, SZO) films are deposited on glass substrates employing femtosecond pulsed laser deposition (fs-PLD). XRD results show that all films are crystalline and prefer c-axis growth. 1 wt% Sm is plausible for doping in ZnO and 2 wt% samarium addition results in reaction among impurity and host atoms forming a compound $ZnSm_2O_4$. Higher concentrations lead to defect generation and decline of crystalline quality. AFM results show that surface roughness is increased with samarium incorporation in addition to affecting particle size and shape. These microstructural variations significantly affect the optical transmittance, reflectance and band gap energies of thin films which are calculated using spectroscopic ellipsometry data. Presence of intrinsic defects and extrinsic defects caused by samarium is revealed by Photoluminescence Spectroscopy. Electrical resistivity of SZO films is significantly affected with Sm concentration in nanocrystalline ZnO. These types of films are suitable for use in optical devices for UV and blue emission.

1. Introduction

ZnO is a semiconductor which is being studied for more than four decades because of its fascinating multiple functional properties. Its wide band gap, high exciton binding energy and ease of availability [1] are mainly responsible for its extensive use in research and application in the fields of optoelectronics, spintronics, piezo-electricity and biomedical engineering [2–5]. The knowledge of nanoscience in material processing and fabrication lead to the popularity of nanostructured and nanocrystalline thin films. As these films can give not only replacement of bulk properties but sometimes reveals new features based on size effects [6–8]. ZnO based nanostructures have gained much attention when doped with rare-earth metals [9]. The optical and electrical properties of the doped ZnO nanoparticles give rise to temperature-stable visible emissions at distinct wavelengths [10–13]. In this context, samarium doped ZnO is grown in the form of nanoparticles and thin films to study the effect of particle size and samarium content on optical and electrical properties of these nanostructures [14–16]. It was determined in the latest work of H.Y. He et al. that optical and electrical properties are strongly affected by the samarium doping [17]. In their study highest Sm concentration used was 1 at.% and at this value the optical transmittance and electrical resistivity of Sm-ZnO thin films reported to decline because of electron-impurity interactions. However, it is important to study the effect of higher samarium concentration on different properties of Sm-ZnO system as these types of films are potential candidate for future generation photovoltaic devices [18]. Therefore, 1–5 wt% Sm is added in ZnO to fabricate SZO thin films in the present research.

Different physical and chemical methods can be used for the deposition of thin films, among which pulsed laser deposition (PLD) is a notable physical vapor deposition technique as it provides variety of parameters to play with for the growth of crystalline or non-crystalline thin films with a promise of conserved stoichiometry [19]. The device fabrication on flexible substrates (organic

* Corresponding author. Laser and Optronics Centre, Department of Physics, University of Engineering & Technology, Lahore 54890, Pakistan.
E-mail address: jaweria04@gmail.com (J.Z. Hashmi).

https://doi.org/10.1016/j.jallcom.2019.05.347
0925-8388/

polymers) and industrial use require low temperature deposition that can be achieved using PLD at room temperature [20]. Therefore a fs pulsed, regenerative amplified Ti:sapphire laser is used in the present research to fabricate samarium doped ZnO thin films at room temperature by using optimized PLD parameters [21]. Effect of samarium concentration on the structural, optical and electrical properties is investigated by analyzing the phase, topography, optical response, photoluminescence and electrical resistivity of these thin films.

2. Experiment

Sm-ZnO films were deposited on well cleaned borosilicate glass substrates (3 cm × 2 cm × 0.1 cm) using fs-PLD. Disc shaped pellets containing 0, 1, 2, 3, 4 and 5 wt% Sm in ZnO prepared using solid state reaction method were used as target materials and ablated using focused femtosecond laser beam (Coherent Libra, Wavelength = 800 nm, Energy per pulse = 180 μJ and pulse duration = 100 fs, Repetition rate = 1 kHz) for deposition. Substrate was mounted parallel to target surface at a distance of 8 cm. Target and substrate were rotated simultaneously at the constant speed of 40 rpm and 20 rpm respectively. PLD chamber was evacuated down to 10^{-5} Torr prior to deposition. During deposition oxygen ambient was maintained at 1 mTorr. All deposition runs were carried out at 25 °C for 1 h. The samples prepared were labeled as SZO-0, SZO-1, SZO-2, SZO-3, SZO-4 and SZO-5 for 0, 1, 2, 3, 4 and 5 wt% samarium doped ZnO thin films respectively.

The as deposited films are characterized for structural properties using X-ray diffraction data measured using Philips X'Pert MPD diffractometer. Surface topography is studied using atomic force microscope (Model: Veeco, di Innova 7.00). Optical transmittance, reflectance, optical constants n and k are measured using spectroscopic ellipsometer (Model: J. A. Woolam M-2000). This optical data is used to calculate optical bandgap energy. Photoluminescence spectra was obtained from an Edinburgh Instruments FLS920 spectrophotometer using Xenon lamp as excitation light source. Electrical resistivity of thin films is measured using four-point probe apparatus (Model: Keithley 4200-SCS).

3. Results and discussions

3.1. Phase analysis

XRD spectrum of 0, 1, 2, 3, 4 and 5 wt% SZO thin films is shown in Fig. 1. It is observed that all the films are crystalline in nature. The observed data is compared with standard reference for wurtzite ZnO using ICDD 00-036-1451 for phase and structural analysis. The (1 0 0), (0 0 2) and (1 1 0) planes of ZnO are identified in undoped ZnO at 31.57°, 34.04° and 55.74° respectively. The intensity of peak corresponding to (0 0 2) plane is maximum with a FWHM value of 0.69° exhibiting preferred c-axis growth of the ZnO thin film. In SZO-1 the (0 0 2) peak is observed at lower Bragg's angle which indicates the increase in d-spacing according to Bragg's law ($2d\sin\theta = n\lambda$). As the ionic radius of Sm^{+3} (0.96 Å) is larger than Zn^{+2} (0.74 Å), so substitution of zinc with samarium at lattice site should increase the d-spacing of ZnO which shifts the xrd peak to lower Bragg's angle. Increasing samarium content to 2 wt%, transforms the single phase ZnO film into a complex solid solution. This change in phase is indicated in Fig. 1 by decrease in intensity of (0 0 2) peak and appearance of new peaks corresponding to Sm_2ZnO_4. The decreased intensity of (0 0 2) peak shows degradation of ZnO hexagonal structure which is attributed to incorporation of samarium atoms and displacement of Zn atoms at interstitial sites. The appearance of strong peak of cubic Sm_2ZnO_4, a compound

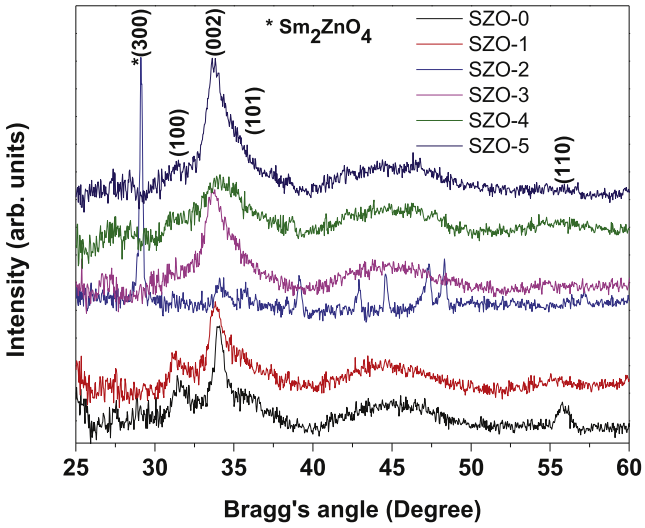

Fig. 1. XRD spectra of 0, 1, 2, 3, 4 and 5 wt% samarium-ZnO thin films.

phase is another reason for the degradation of ZnO regular hexagonal structure. The appearance of zinc samarium oxide in Sm-doped ZnO system is a first-time observation according to our knowledge. According to Morris, in a solid solution the concentration and the chemical properties of solute both are significant in defining the phase segregation (decomposition) and compound ordering in a solid solution [22]. If the solute (here the dopant) atoms prefer bonding with each other then, there solubility is limited and they tend to make clusters leading to phase segregation. On the other hand, if the solute atoms prefer to bond with solvent atoms, they adopt ordered configurations in a regular crystal pattern. This ordered growth can lead to phase separation between solvent and the ordered compound depending upon concentration of solute. In the present study as the concentration of samarium is changed, both situations are observed. The solubility of samarium in ZnO is limited because it has larger ionic radius (0.96 Å) and different valency (+3) than Zn (ionic radius = 0.74 Å and valency = +2). Therefore, only 1 wt% samarium is plausible for doping in ZnO. In SZO-2 the samarium content is increased and $ZnSm_2O_4$ compound is formed which indicates ordered layered growth of the host (solvent) and dopant (solute) atoms. In SZO-3, the disappearance of compound phase indicates a more complex situation. Now a look on electronegativity values of Sm (1.17), Zn (1.65) and O (3.44) can give one of the reasons behind this complex situation. Samarium zinc oxide, Samarium oxide and Zinc oxide are all stable phases. So, all these phases are likely present in these thin films. The crystalline growth of these phases depends on film deposition and growth conditions. The femto-PLD is famous for nanocrystalline thin films. Therefore, wurtzite ZnO phase is observed with poor crystallinity in SZO-3, SZO-4 and SZO-5, as this is the major phase quantitatively which can be grown at room temperature (26 °C) using femto PLD [18]. The other phases are present in amorphous form and re-appear in their crystalline form when samarium content is increased to 10 wt%.

The 2θ values and FWHM of (0 0 2) peak of all SZO films are given in Table 1. The broadening indicates increased disordering with increasing samarium concentration. Thus, the limited solubility of samarium in ZnO is the key factor responsible for point defects like vacancy, interstitial, substitutional and grain boundary due to phase segregation when Sm content is increased to 5 wt%. This analysis suggests that only 1 wt% samarium can be doped in ZnO without substantial deformation of its hexagonal structure or

Table 1
The XRD data and roughness values of samarium zinc oxide thin films.

Sample Name	Sm. Content	(002) position	(002) FWHM	Identified Phases	Crystallite size	Roughness (AFM)	
						rms	avg
	at. %	(°)	(°)		nm	nm	nm
SZO-0	0	34.04	0.69	ZnO	15	6.1	4.8
SZO-1	1	33.86	0.97	ZnO	10	17.8	14.7
SZO-2	2	34.15	0.84	ZnO, Sm_2ZnO_4	12	8.6	6.9
SZO-3	3	33.74	2.44	ZnO	4	9.7	7.1
SZO-4	4	34.04	3.13	ZnO	3	6.5	4.4
SZO-5	5	33.74	2.29	ZnO	4	12.5	10.5

formation of a new phase. Co-existence of different phases give rise to several structural defects as mentioned above, which are significant for determining the optical and electrical properties.

3.2. Topography

The surface of samarium doped ZnO thin films is examined with Atomic Force Microscope and the selected 2D micrographs of $1 \times 1\ \mu m^2$ area of each SZO thin film are presented in Fig. 2. It is inspected that the undoped ZnO film shown in Fig. 2a is made up of uniformly distributed small elongated grains of widths 25–70 nm and lengths 90–100 nm. 1, 2, 3, 4 and 5 wt% SZO thin films are shown in Fig. 2 b to Fig. 2f respectively. Fig. 2b shows the amalgamation of elongated grains in 1 wt% SZO thin film, like the results of cadmium doped ZnO [23]. In 2 wt% SZO they change into closely packed, distinguishable spherical grains (Fig. 2c). Further increase in samarium content to 3 wt% disintegrates the uniformly deposited thin film into separate regions of smaller grains and nucleated

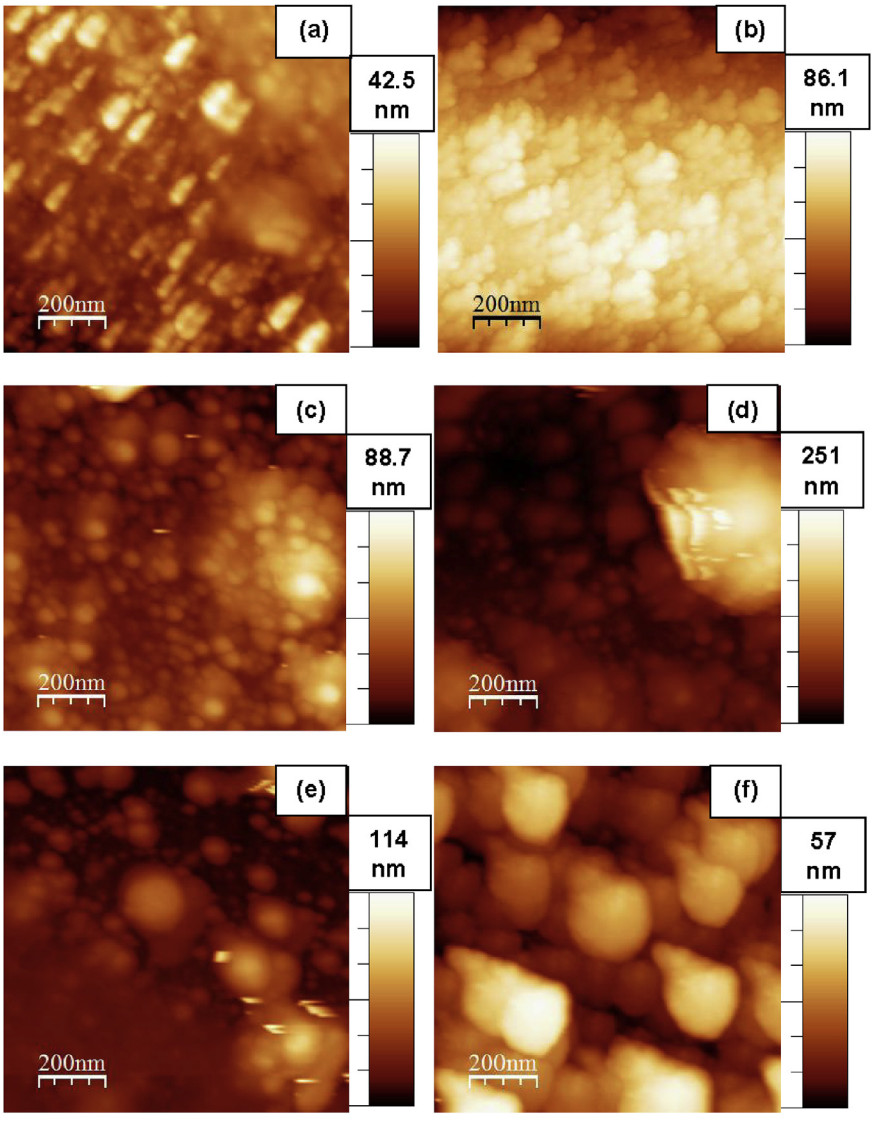

Fig. 2. Atomic Force Micrographs of samarium zinc oxide thin films containing different samarium content. (a) 0 wt%, (b) 1 wt%, (c) 2 wt%, (d) 3 wt%, (e) 4 wt% and (f) 5 wt%.

larger grains separated by voids as shown in Fig. 2d. This variation in size of surface grains and their distribution keeps on changing with increase in amount of samarium.

The root mean square roughness is a parameter calculated from AFM micrographs to comment on the quality of thin films surface. Here rms roughness is calculated using WSxM software [24] and the values are given in Table 1. It is found that the roughness increases non-linearly with samarium concentration, giving smallest value 6.1 nm for undoped ZnO and highest value 17.8 nm for SZO-1. This random variation of roughness can be related to crystallite size calculated from XRD data. Roughness varies contrary to crystallite size variation from 0 to 2 wt%. With increase in Sm concentration from 3 to 5 wt%, roughness increases irrespective of crystallite size. This increase in roughness results from long range disorder caused by existence of amorphous Sm_2ZnO_4 and Sm_2O_3.

3.3. Optical properties

3.3.1. Spectroscopic ellipsometry

Optical transmittance, reflectance, refractive index and extinction coefficient of SZO thin films as a function of wavelength are presented in Fig. 3a, b, c and d respectively. All SZO films show low transmittance in the range 250–380 nm and are transparent in range 380 nm–1000 nm of electromagnetic spectrum. The transmittance of undoped ZnO is 75% at 600 nm which reduces to 60% with incorporation of 1 wt% Sm in ZnO and increases to 80% for SZO-2. With further increase in Sm quantity the %T varies randomly showing minimum value of 45% for 3 wt% and maximum value of 80% for 4 wt% SZO. The transmittance is reduced at lower samarium values because of substitutional defects. Substitution of Sm^{+3} in place of Zn^{+2}, offers one extra electron per bond as samarium acts as a donor impurity in ZnO. These extra charge carriers reduce the transmittance by photon-impurity interaction. On the other hand, at higher concentrations, transmittance decreases due to the presence of structural disorder caused by amorphous phases. These amorphous phases increase grain boundary scattering and reduce transmittance. Interestingly higher transmittance is observed in thin films which contain samarium zinc oxide compound. This behavior may be attributed to high atomic ordering in these thin films.

Reflectance of all SZO thin films is high in the wavelength range of 300–600 nm and it decreases with increasing wavelength regardless of samarium doping. 1 wt% samarium decreases reflectance from 10% to 7% and also blue shifts the reflectance peak. Increase in samarium content from 2 to 5 wt% increases the reflectance values close to undoped ZnO. Reflectance from a thin film depends on many factors including its surface morphology, structure formation underneath the surface and concentration of free carriers. In SZO thin films, the samarium doping induce modification in all these three parameters therefore, reflectance of film varies randomly at higher (>2 wt%) Sm content.

The refractive index (n) of undoped ZnO thin film (SZO-0) is 2.2 at 600 nm which is close to the reported value [25]. n decreases from 2.2 to 2 and 1.9 when 1 and 2 wt% samarium is added respectively. This decrease is attributed to photon-impurity interaction. The substitution of Sm ions at Zinc sites results in the increase of interplanar spacing which reduces the density and refractive index [26]. At higher samarium concentrations (3, 4, and 5 wt%) n varies randomly, showing values always lower than 2.2. This shows that the refractive index of SZO thin film is dependent on samarium content as it modifies the structure and surface morphology of thin films by creating defects.

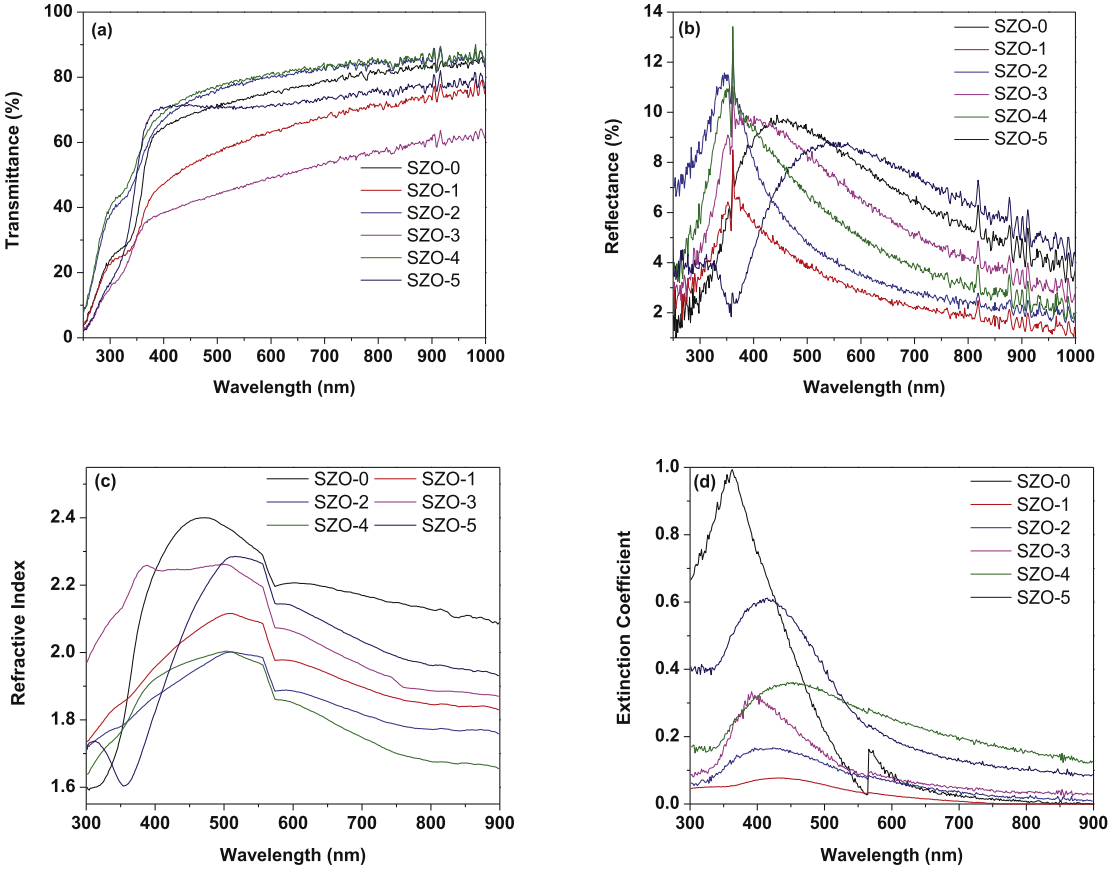

Fig. 3. Optical data of Sm-ZnO thin films. (a) transmittance, (b) reflectance, (c) refractive index and (d) extinction coefficient.

Energy loss of electromagnetic radiation inside the thin film is determined from extinction coefficient (k). These losses can occur due to scattering and absorption of light. Fig. 3d shows the extinction coefficient of all SZO thin films in the wavelength range 300–900 nm. The values of 'k' are highest in 300–500 nm range and then k decreases with increasing wavelength from 500 nm to 900 nm for all SZO thin films. The high values of k from 300 to 500 nm are due to light absorption for band edge transitions. The red shift of this absorption edge shows decrease in bandgap whereas blue shift indicates increase in bandgap. A red shift in absorption edge is observed in all thin films containing samarium as shown in Fig. 3d. This indicates availability of energy levels below conduction band contributing in radiative transitions. Donor levels are expected to be formed in SZO-1 as samarium is an electron-donor impurity so, its replacement in Zn site will generate energy level below conduction band. Increased amount of samarium in SZO-2 and SZO-3 results in blue-shift of this absorption edge as compared to SZO-1. This indicates saturation of impurity atoms and phase segregation. Also, from XRD analysis, the presence of zinc samarium oxide compound in SZO-2 will result in change of energy levels for electronic transition. A random variation in behavior of extinction coefficient as a function of samarium content in rest of the samples suggests strong dependence on material's structure.

To further investigate the role of structural defects on optical properties of SZO thin films, the optical band gap energy E_g of SZO thin films is calculated from the Tauc's curves and the values are given in Table 2. Highest E_g value 2.97 eV is obtained for undoped ZnO which is smaller than the bulk value (3.37 eV) but this value is closer to the optical bandgap of nanostructured ZnO thin film reported in literature [27]. The E_g value lowers to 2.34 eV when 1 wt% Sm is added in ZnO indicating energy states below the conduction band as already stated. Further increase in samarium content (2 and 3 wt%) increases the optical band gap to 2.63 eV. Lowest value of E_g is observed for SZO-4, which shows presence of some deep level defect states within the forbidden energy gap. It can be seen from Fig. 1 that crystalline quality of SZO-4 is very poor indicating the high structural disorder. This disorder is observed when amorphous phases are present in a material. But as XRD does not give details of amorphous phases so optical spectroscopy is used to analyze nature of thin film material through optical properties. Therefore, the band gap value of SZO-4 confirms presence of pure and compound phases of zinc and samarium oxide in amorphous form. E_g value increases again in SZO-5 with improvement in crystalline phase. All these E_g values are lower than the undoped ZnO which can be attributed to the variation in structural disorders caused by re-arrangement of atoms and presence of multiple phases giving rise to various defect states.

3.3.2. Photoluminescence

The photoluminescence spectrum of SZO thin films is shown in Fig. 4. All films show a broad fluorescence emission band in the spectral range of 350–450 nm which is deconvoluted using OriginPro. 9 software. An illustration of deconvolution of SZO-5 is given in Fig. 4b. The emission wavelengths from the deconvoluted data are given in Table 2. Undoped ZnO gives emission in the UV at 374 nm (3.32 eV) and 384 nm (3.23 eV) which are generally attributed to ultraviolet band edge emissions from ZnO originating from free exciton recombination and free electron-to-acceptor recombination [28]. With incorporation of Sm^{+3} ions in ZnO slight red shifts of emission wavelengths of UV band is observed confirming results of spectroscopic ellipsometry. Apart from UV band (band edge transitions), three other bands are observed in samples containing 2–5 wt% Sm at ~356 nm (3.48 eV), 410 nm (3.02 eV) and 490 nm (2.53 eV). The 356 nm band is observed in intrinsic ZnO by D.H. Zhang et al. and they interpreted it as quasi-fermi level shift in to conduction band [29]. Other observations of photoemission higher than bandgap energy of ZnO are also present [30]. In our case this emission is observed in the samples containing $ZnSm_2O_4$ which shows high absorption in UV (~237 nm) [31], therefore we

Table 2
Data obtained from optical and electrical analysis of Sm-ZnO thin films.

Sm. Content	Optical Band Gap	Emission wavelengths from PL	Electrical Resistivity
at. %	eV	nm	Ω-cm
0	2.97	374.4, 384.4	0.34
1	2.34	375.7, 385.3, 489.2	0.22
2	2.4	353.3, 377.5, 411.2, 461.5	1.23
3	2.63	355.7, 379.9, 415.5, 484.4	1.96
4	2.14	359.4, 383.4, 383.7, 495.2	2.48
5	2.41	356.2, 378.4, 411.7, 487.9	0.40

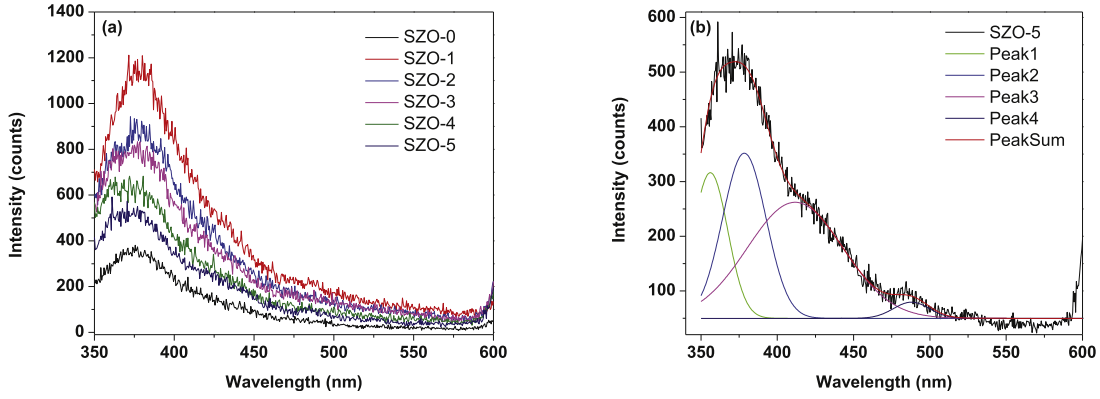

Fig. 4. Photoluminescence spectrum of samarium-ZnO thin films. (a) Photoemission of all Sm-ZnO thin films as a function of samarium content. (b) deconvolution of PL data obtained for SZO-5.

interpret this high-energy emission as a result of charge transition between ZnO valence band and some samarium-zinc related defect within conduction band of ZnO. The violet emission (~410 nm) and blue-green emission (~490 nm) are related to defects like traps caused by grain boundaries in nanostructured ZnO films or interface present between different phases as per detailed discussion in the research of Shabnam et al. [32]. In our study these reasons are supported by XRD and AFM results which show that crystallite size is very small that increases number of grain boundaries. Furthermore, the samarium ions and atoms are also considered responsible for deep level emissions in SZO thin films because our previous work on undoped ZnO thin film using similar conditions of femto-PLD [21] did not show these VISIBLE range emission wavelengths. Therefore, the shift in these emission wavelengths based on samarium content is attributed to variation in Sm-Zn based complex phase which significantly contributes in radiative transitions. The band emission at 470 nm is also observed due to samarium ions in borate glasses [33] known as $^4G_{5/2}$ to $^6H_{5/2}$ radiative transition. In case of femtosecond PLD, energetic particles may adsorb at substrate surface and in that case emission from embedded Sm ions is also possible subject to penetration depth of incident light used to observe PL. But this is merely a possibility as penetration depth is not known in our case.

3.4. Electrical measurements

The I-V data of SZO thin films with samarium content varying from 0 to 5 wt% is obtained using Four-point probe apparatus containing 40 different values of current and voltage. This data is used to calculate average resistivity ρ of all thin films using equation (1).

$$\rho = \frac{\pi}{ln2} \times t \times \frac{V}{I} \quad (1)$$

Where V is the voltage applied in volts, I is the measured current in amperes, t is film thickness and $(\pi/\ln 2)$ is the correction factor [34].

The obtained values of resistivity are given in Table 2. The transport properties of a thin film depend on material of film as well as its growth mechanism [17]. The resistivity of undoped ZnO thin film is ~0.34 Ω-cm which decreases to 0.22 Ω-cm with incorporation of 1 wt% samarium. This decrease is attributed to expected increase in carrier concentration upon substitution of trivalent Sm^{+3} in place of Zn^{+2} at lattice site. Further increase in samarium content from 2 to 4 wt% increases average resistivity of SZO films. This change is correlated with crystallite size given in Table 1. The comparison of crystallite size and resistivity values shows that films with smaller size grains have high resistivity. As stated earlier, femto-PLD is known for fabrication of nanocrystalline thin films. The nanocrystalline growth of material results in increased grain boundary defect. So, the resistivity of these films is generally higher. In present case this effect is further enhanced by the presence of multiple impurity phase. Similar observation is reported for Ni doped ZnO [35], where charge transport in polycrystalline film is explained on the basis of GB model. According to this model, a potential barrier is created around grain boundary due to bending of energy bands when electrons are trapped in surface states. As a result, grain boundary scattering significantly increases the resistivity for smaller grains.

4. Conclusions

Samarium zinc oxide thin films are successfully deposited with varying samarium concentration from 0 to 5 wt% on borosilicate glass substrates. XRD results show that only 1 wt% Sm is plausible for doping in ZnO. Higher concentration of samarium supports formation of zinc samarium oxide compound and structural defects which significantly affect the optical and electrical properties. The surface topography demonstrates that samarium doping strongly effects the particle size, shape and average roughness of thin films. Optical transmittance, optical band gap and luminescence are also consistent with structural deviations with samarium addition. Sm incorporation affects the charge density and particle size which is substantial to control the electrical resistivity of these nanocrystalline thin films.

It is concluded that rare-earth impurity like samarium in nanocrystalline ZnO can be adjusted quantity wise along with deposition technique, the femto-PLD for the controlled modification in optical and electrical response of ZnO thin films. Therefore, these type of films can be used for photovoltaic applications and thin film based UV–visible emissive devices.

Acknowledgements

Jaweria Zartaj Hashmi is grateful to Higher Education Commission of Pakistan (Project: "IRSIP", PIN: IRSIP 27 PS 22) for their International Research Support Initiative Program (IRSIP). Authors also acknowledge EPRSC of the UK (project “SEAMATICS”, EP/M015165/1).

References

[1] C. Klingshirn, J. Fallert, H. Zhou, J. Sartor, C. Thiele, F. Maier-Flaig, D. Schneider, H. Kalt, 65 years of ZnO research – old and very recent results, Phys. Status Solidi B 247 (6) (2010) 1424–1447.
[2] A.B. Djurisic, A.M.C. Ng, X.Y. Chen, ZnO nanostructures for optoelectronics: material properties and device applications, Prog. Quant. Electron. 34 (2010) 191–259.
[3] J. Zhang, X.Z. Li, J. Shi, Y.F. Lu, D.J. Sellmyer, Structure and magnetic properties of Mn-doped ZnO thin films, J. Phys. Condens. Mater. 19 (036210) (2007) 1–8.
[4] E. Lee, J. Park, M. Yim, Y. Kim, G. Yoon, Characteristics of piezoelectric ZnO/AlN-stacked flexible nanogenerators for energy harvesting applications, Appl. Phys. Lett. 106 (023901) (2015) 1–5.
[5] S.K. Arya, S. Saha, J.E. Ramirez-Vick, V. Gupta, S. Bhansali, S.P. Singh, Recent advances in ZnO nanostructures and thin films for biosensor applications: Review, Anal. Chim. Acta 737 (2012) 1–21.
[6] Ion Tiginyanu, Pavel Topala, Veaceslav Ursaki (Eds.), Nanostructures and Thin Films for Multifunctional Applications Technology, Properties and Devices, Springer, 2016, https://doi.org/10.1007/978-3-319-30198-3.
[7] O. Dobrozhan, D. Kurbatov, P. Danilchenko, A. Opanasyuk, Nanostructured ZnO, Cu2ZnSnS4, Cd1−xZnxTe thin films obtained by spray pyrolysis method, in: Inguanta Rosalinda, Sunseri's Carmelo (Eds.), Semiconductors - Growth and Characterization, 2018, https://doi.org/10.5772/intechopen.72988.
[8] M. Laurenti, V. Cauda, Porous Zinc Oxide Thin Films: Synthesis Approaches and Applications, Coatings 8 (2018) 67 1–6724, https://doi.org/10.3390/coatings8020067.
[9] J.Z. Hashmi, K. Siraj, S. Naseem, S. Shaukat, Dopant-induced modifications in structural and optical properties of ZnO thin films prepared by PLD, Mater. Res. Express 3 (096402) (2016) 1–12.
[10] Y. Yang, Y. Li, C. Wang, C. Zhu, C. Lv, X. Ma, D. Yang, Rare-earth doped ZnO films: a material platform to realize multicolor and near-infrared electroluminescence, Adv. Opt. Mater. 2 (2014) 240–244.
[11] F. Wu, L. Fang, Y.J. Pan, K. Zhou, H.B. Ruan, G.B. Liu, C.Y. Kong, Effect of annealing treatment on structural, electrical, and optical properties of Ga-doped ZnO thin films deposited by RF magnetron sputtering, Thin Solid Films 520 (2011) 703–707.
[12] Y. Chen, X.L. Xu, G.H. Zhang, H. Xue, S.Y. Ma, Blue shift of optical band gap in Er-doped ZnO thin films deposited by direct current reactive magnetron sputtering technique, Physica E 42 (2010) 1713–1716.
[13] R. Kaur, A.V. Singh, R.M. Mehra, Physical properties of natively textured yttrium doped zinc oxide films by sol-gel, J. Mater. Sci. Mater. Electron. 16 (2005) 649–655.
[14] K.G. Nair, K.P. Mani, V. George, P. Chandran, C. Joseph, V.P.N. Nampoori, Nonlinear optical characterization of samarium doped zinc oxide nanoparticles, in: Proceedings of National Laser Symposium (NLS-21), BARC, Mumbai, Feb 2013, pp. 6–9.
[15] S. Chawla, M. Saroha, R.K. Kotnala, White light emitting magnetic ZnO:Sm nanoparticles prepared by inclusive co-precipitation synthesis, Electron Mater. Lett. 10 (1) (2014) 73–80.
[16] T.P. Rao, S.G. Raj, M.C.S. Kumar, Optical properties of samarium doped ZnO thin films, in: 2nd International Conference on Devices, Circuits and Systems

(ICDCS), IEEE, 2014, pp. 1–4.
[17] H.Y. He, J. Fei, J. Lu, Sm-doping effect on optical and electrical properties of ZnO thin films, J. Nanostruct. Chem. 5 (2015) 169–175.
[18] M. Novotný, E. Marešová, P. Fitl, et al., The properties of samarium-doped zinc oxide/phthalocyanine structure for optoelectronics prepared by pulsed laser deposition and organic molecular evaporation, Appl. Phys. A 122 (225) (2016) 1–8.
[19] R. Eason, Pulsed Laser Deposition of Thin Films: Applications-Led Growth of Functional Materials Willey, 2007 (New Jersey).
[20] K. Tian, B. Tudu, A. Tiwari, Growth and characterization of zinc oxide thin films on flexible substrates at low temperature using pulsed laser deposition, Vacuum (2017). https://doi.org/10.1016/j.vacuum.2017.01.018.
[21] J.Z. Hashmi, K. Siraj, A. Latif, M. Murray, G. Jose, Study of deposition parameters for the fabrication of ZnO thin films using femtosecond laser, Appl. Phys. A 122 (763) (2016) 1–10.
[22] Morris JW, Jr Materials Science Chapter 4: Defects in Crystals, pg 82.
[23] A. Fouzri, M.A. Boukadhaba, A.H. Taure, N. Sakly, A. Bchetnia, V. Sallet, Structural, morphological, optical and electrical properties of Zn(1-x) CdxO solid solution grown on a- and r-plane sapphire substrate by MOCV, J. Cryst. Process Technol. 3 (2013) 36–48.
[24] I. Horcas, R. Fernández, J.M. Gómez-Rodríguez, J. Colchero, J. Gómez-Herrero, A.M. Baro, WSXM: a software for scanning probe microscopy and a tool for nanotechnology, Rev. Sci. Instrum. 78 (013705) (2007) 1–8.
[25] C. Gumus, O.M. Ozkendir, H. Kavak, Y. Ufuktepe, Structural and optical properties of zinc oxide thin films prepared by spray pyrolysis method, J. Optoelectron. Adv. Mater. 8 (1) (2006) 299–303.
[26] M. Ghanipour, D. Dorranian, Effect of Ag-nanoparticles doped in polyvinyl alcohol on the structural and optical properties of PVA films, J. Nanomater. 2013 (897043) (2013) 1–10.
[27] M. Shaban, M. Zayed, H. Hamdy, Nanostructured ZnO thin films for self-cleaning applications, RSC Adv. 7 (2017) 617–631.
[28] Y.M. Lu, X.P. Li, P.J. Cao, S.C. Su, F. Jia, S. Han, W.J. Liu, D.L. Zhu, X.C. Ma, Study of ultraviolet emission spectra in ZnO thin films, J. Spectrosc. 1 (2013) 1–7.
[29] D.H. Zhang, Q.P. Wang, Z.Y. Xue, Photoluminescence of ZnO films excited with different wavelength, Appl. Surf. Sci. 207 (2003) 20–25.
[30] Y. Wang, B. Chu, Structural and optical properties of ZnO thin films on (111) CaF_2 substrates grown by magnetron sputtering, Superlattice. Microst. 44 (2008) 54–61.
[31] L.R. Damiani, R.D. Mansano, Zinc oxide thin films deposited by magnetron sputtering with various oxygen/argon concentrations, J. Phys. Conf. Ser. 370 (012019) (2012) 1–7.
[32] Kant CR. Shabnam, P. Arun, Size and defect related broadening of photoluminescence spectra in ZnO:Si nanocomposite films, Mater. Res. Bull. 47 (2012) 901–906.
[33] A.V. Deepa, M. Priya, S. Suresh, Influence of samarium oxide ions on structural and optical properties of borate glasses, Sci. Res. Essays 11 (5) (2016) 57–63.
[34] B. Nasr, S. Dasgupta, D. Wang, N. Mechau, R. Kruk, H. Hahn, Electrical resistivity of nanocrystalline Al-doped zinc oxide films as a function of Al content and the degree of its segregation at the grain boundaries, J. Appl. Phys. 108 (103721) (2010) 1–6.
[35] A. Yildiz, B. Kayhan, B. Yurduguzel, A.P. Rambu, F. Iacomi, S. Simon, Ni doping effect on electrical conductivity of ZnO nanocrystalline thin films, J. Mater. Sci. Mater. Electron. 22 (2011) 1473–1478.